Synthetic Preparations and Physical and Electrical Properties of Main Chain Type Thermotropic Liquid Crystalline Polyimide/SiO_2 Nanocomposites

Czung-Yu Ho, Jiunn-Yih Lee

Department of Polymer Engineering, National Taiwan University of Science and Technology, Taipei 10607, Taiwan, Republic of China

Received 3 March 2005; accepted 5 August 2005
DOI 10.1002/app.23627
Published online in Wiley InterScience (www.interscience.wiley.com).

ABSTRACT: Two kinds of monomers, 1,3-bis[4-(4′-amino-Phenoxy)cumyl]benzene (BACB) and pyromellitic dianhydride were used to synthesize the Liquid Crystalline Polyamic acid—a precursor (LCPAA) of Liquid Crystalline Polyimide (LCPi). The nanohybrid films were successfully prepared by the sol–gel reaction. Tetraethoxysilane (TEOS) (99%)–ethanol (99.8%) solution was added to LCPAA solution. The hybrid films were made by the hydrolysis–polycondensation of TEOS–ethanol in the LCPAA solution. When water and the solvent were removed completely, the hybrid films were obtained. The functional group and chemical structure were characterized by FTIR. We employed a number of instruments to understand whether the nano-SiO_2 particle was introduced into the polymer matrix and enhanced the thermal properties and mechanical strength. The liquid crystalline phase of the LCPi and LCPi/SiO_2 hybrid films was observed by POM. TGA and DSC were used to test the thermal properties. The crystallization and liquid crystal phase analyses were carried out by XRD. The elemental analysis was employed to measure the 1,3-bis[4-(4′-nitrophenoxy)cumyl)]benzene and BACB monomers. Besides, the cross section at morphology of the materials was observed with an FESEM. The electrical properties of hybrid films were measured by the high resistance analysis and dielectric constant analysis. J Appl Polym Sci 100: 1688–1704, 2006

Key words: polyimide; sol–gel reaction; polycondensation; hybrid films; crystallization

INTRODUCTION

The main-chain-type thermotropic liquid crystalline polymers (TLCPs) have already been established as high performance commercial engineering polymers. This is due to their specific chemical structure, high strength, high modulus (especially if measured in the direction of molecular alignment), excellent properties at high working temperatures, low viscosities, low coefficient of thermal expansion, good dielectric characteristics, and good mechanical properties. Liquid crystalline order is exhibited by LCPs in the melt (thermotropic LCPs), because of the rigid character of the molecules, or in the solution (lyotropic LCPs). In main-chain LCPs, the rigid groups are parts of the polymer chains, while in side-chain LCPs they are attached to a (flexible) polymer backbone. Main-chain LCPs are potentially useful materials, as the molecular orientation enables the development of strong products. The melting point of lyotropic LCPs is above their decomposition temperature, and so they can be processed only from a solution. The melting point of thermotropic LCPs is lower, and so they can be processed from the melt. Because of this advantage, TLCPs are widely used in aerospace and electronics. These applications approach the limits of thermal stability, hence an understanding of the factors influencing the thermal stability of TLCPs is important.[1–8] They have been widely used in electronic devices, microelectronic packaging, structural composites, and membrane devices.[9] Although wholly aromatic TLCPs exhibit very attractive mechanical properties, it is difficult for them to process.[10]

Polyimides (PIs) are types of high performance polymeric materials that have been widely used in the aerospace, electronics, and microelectronic industries because of their outstanding thermal and chemical stabilities, mechanical properties (e.g. high tensile strength and modulus), electrical properties (e.g. low dielectric properties), and radiation resistance.[11–15] However, PIs exhibit relatively higher values of water absorption and coefficients of thermal expansion (about 5×10^{-5} k^{-1}). Their competitors for microelectronics are ceramics (silica). Ceramics show lower coefficients of thermal expansion (about 5×10^{-7} k^{-1}) and water absorption,[16] which is very important in electronic applications, for example, in multilayer structures of module chips. So, polyimide/

Correspondence to: J.-Y. Lee (jlee@tx.ntust.edu.tw or D9404201@mail.ntust.edu.tw).

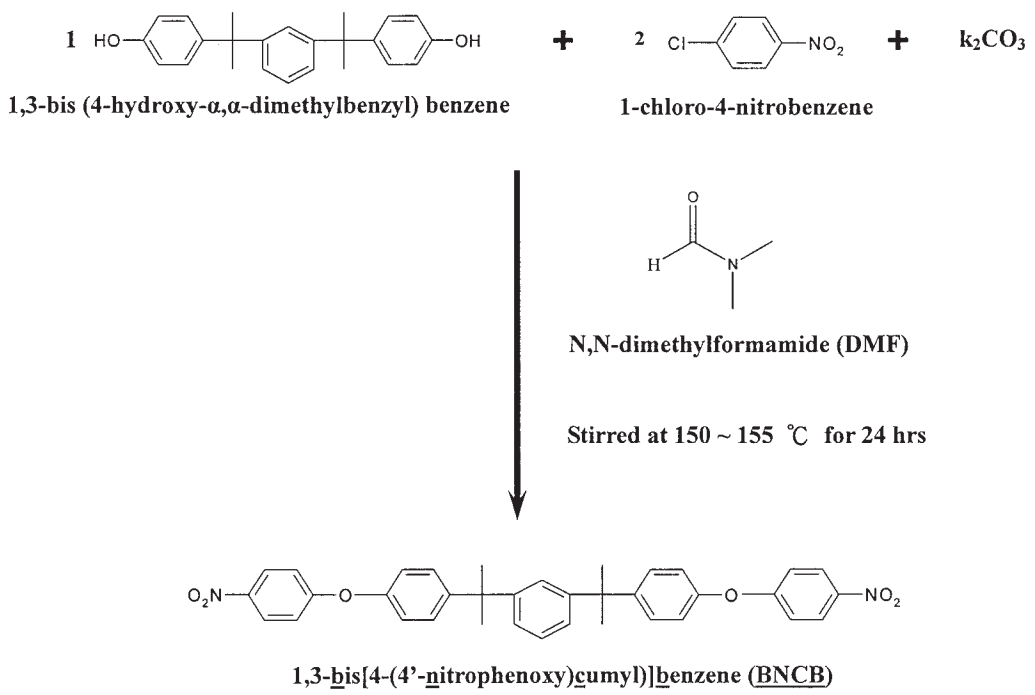

Scheme 1 Synthesis process of BNCB monomer.

SiO_2 hybrids have been developed to combine the extraordinary properties of both organic and inorganic materials.

In the past 3 decades, the sol–gel process has been developed as a method to prepare inorganic metal oxides from an organic metal alkoxide under mild conditions. The network forming from the sol–gel process involves in the simultaneous hydrolysis and condensation of poly (valent) metal alkoxides to produce a gel.[17]

Early in the 1990s, this method was used to prepare PI/SiO_2 hybrids. Nandi et al. made PI/SiO_2 hybrids by mixing the solutions of pyromellitic dianhydride (PMDA), oxydianiline (ODA), and silicon tetraalkoxide. These materials became opaque at a low weight percentage of silica because of phase separation on a

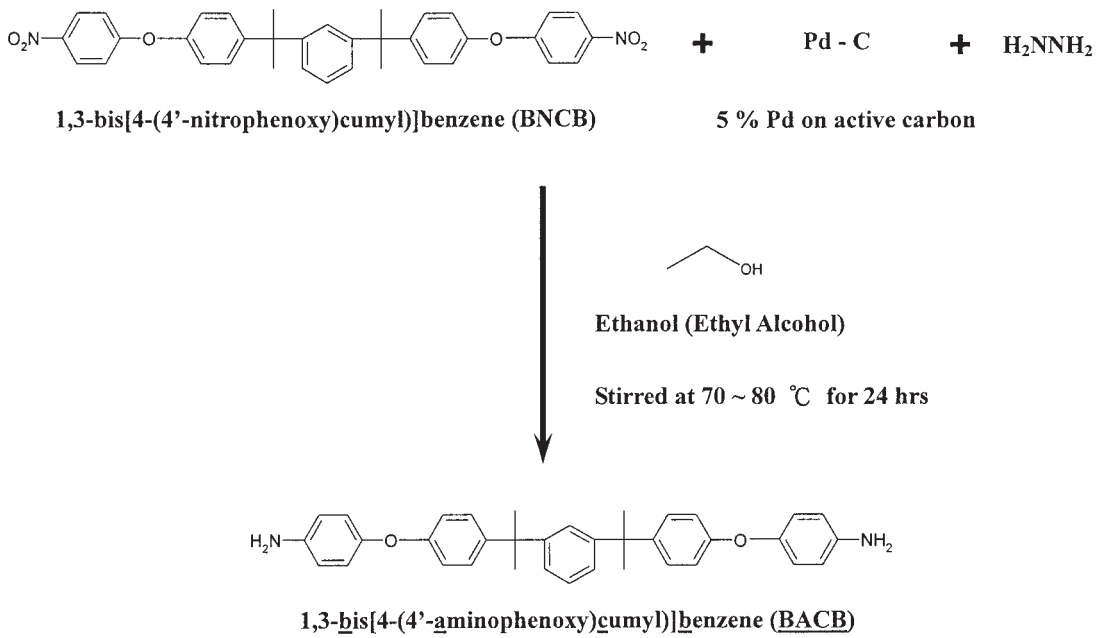

Scheme 2 Synthesis process of BACB monomer.

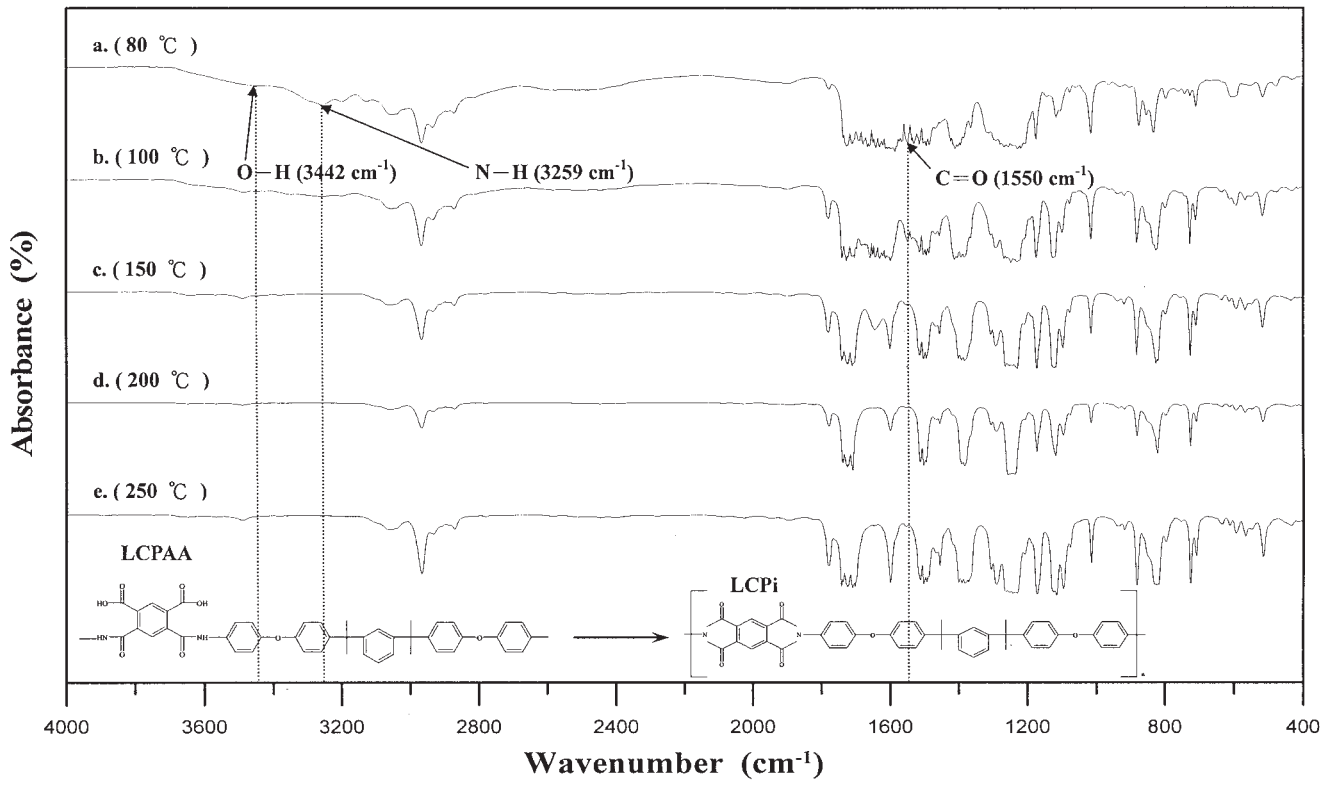

Figure 1 FTIR spectra of pure LCPi film. (a), (b), (c), (d), and (e), after heating at 80, 100, 150, 200, and 250°C for 1 h, respectively.

micrometer scale.[18] Morikawa et al.[19] reported that when the content of silica was more than 8% and when particles bigger than 1 μm were observed, the film became opaque. Sysel and Maryska pointed out that there were only physical interactions between the organic and inorganic phases in the common PI/SiO_2 hybrids.[20]

As the ULSI circuits were scaled down to deep submicron regime, interconnect delay became increasingly dominant over intrinsic gate delay. To reduce the RC delay time, many low dielectric constant materials have been developed.[21] So, in this study, the intrinsic properties of LCPi/SiO_2 were investigated.

In this study, we have successfully completed the preparation of LCPi/SiO_2 nanohybrid materials by the sol–gel process from the hydrolysis–polycondensation of tetraethoxysilane (TEOS) (99%)–ethanol (99.8%) in the liquid crystalline polyamic acid solution. As the condensation reaction of silanol proceeds, the pendent hydroxyl groups may partly crosslink with the silica network, forming a strong interconnection between the organic and inorganic phases. So the hybrids do not show any obvious phase separation down to the nanoscale range when the silica content is less than 6.5 wt %. We employed a lot of instruments to evaluate whether the nano-SiO_2 particle was introduced into the polymer matrix and enhanced the thermal properties and mechanical strength, and reduced the dielectric constant.

TABLE I
Silica Contents of LCPi/SiO_2 Hybrid Materials

Sample no.	LCPAA (g)	TEOS (mL)	Ethanol (mL)	TEOS (wt %)	Silica content[a] (SiO_2 wt %)
1	20	0	0	0	—
2	20	1.1	1.3	5.0	1.5
3	20	2.3	2.7	9.7	3.0
4	20	3.9	4.6	15.4	5.0
5	20	5.2	6.1	19.4	6.5

[a] Silica content was calculated under the assumption that the Sol–Gel reaction proceed completely.

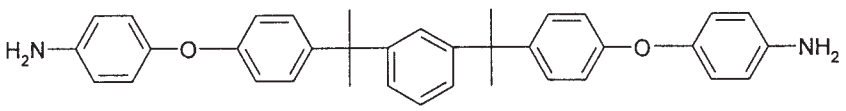

1,3-bis[4-(4'-aminophenoxy)cumyl)]benzene (BACB)

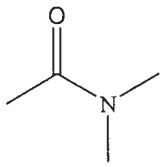

N,N-Dimethylacetamide (DMAC)

Stirred at room temperature for 30 mins ~ 1 hr

Mixing

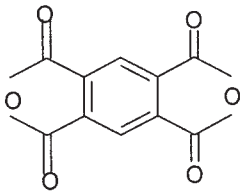

Pyromellitic dianhydride (PMDA)

Stirred at room temperature

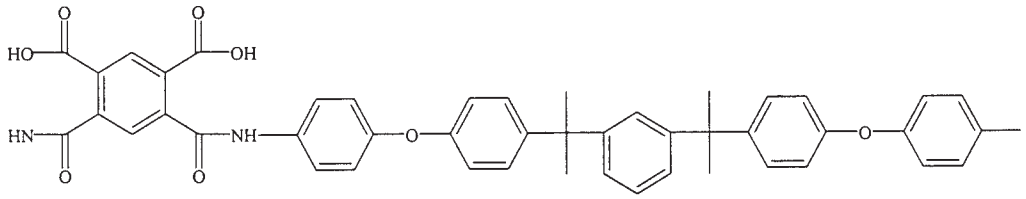

(Liquid Crystalline Poly (amic acid), LCPAA)

Scheme 3 Synthesis process of LCPAA solution.

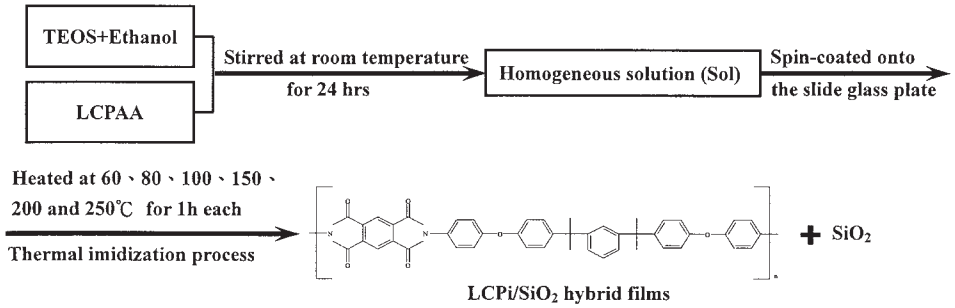

Scheme 4 Preparation of LCPi/SiO_2 hybrid films via Sol–Gel process.

EXPERIMENTAL

Materials

1,3-Bis(4-hydroxy-α,α-dimethylbenzyl)benzene (99%, Aldrich), ethanol (ethyl alcohol) (99.8%, Fluka, Buchs, Switzerland), and tetraethoxysilane (TEOS) (≥99%, Fluka) were purchased from Uni-Onward Co. (Taipei, Taiwan). 1-Chloro-4-nitrobenzene (98+%, Lancaster), potassium carbonate (99.9%, Scharian), ethanol (ethyl alcohol) (99.5%, made in Japan), palladium on activated carbon (5% Pd, Acros), and potassium bromide (IR grade 99+%, Acros) were purchased from Dinhaw Enterprise Co. (Taipei, Taiwan). *N*,*N*-dimethylformamide (DMF) (99.98%, Tedia), *N*,*N*-dimethylacetamide (DMAC) (Tedia), *d*-chloroform (99.8 Atom% D, Acros), and hydrazine monohydrate (98+%, TCI) were purchased from Echo Chemical Co. (Taipei, Taiwan). Pyromellitic dianhydride (PMDA) (99%) was obtained from Tai-Flex Scientific Co. (Kaohsjung, Taiwan)

Synthesis of 1,3-bis[4-(4′-nitrophenoxy)cumyl)]benzene (BNCB)

A 1000-mL one-necked round-bottom flask containing 17.32 g (0.05 mol) of 1,3-bis(4-hydroxyl-α,α-dimethylbenzyl)benzene, 17.33 g (0.11 mol) of 1-chloro-4-nitrobenzene, 8.29 g (0.06 mol) of potassium carbonate, and 200 mL of DMF was fitted with a mechanical stirrer and a reflux condenser. The mixture was heated and

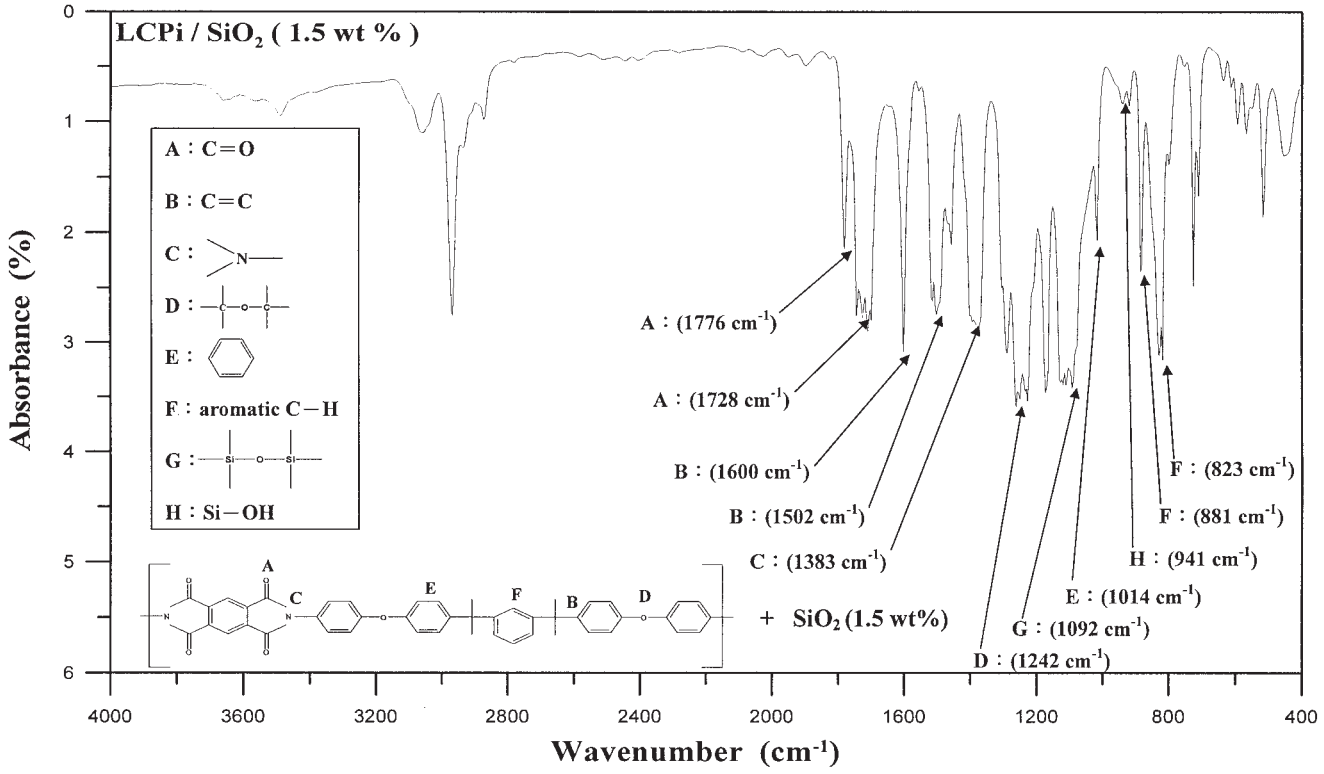

Figure 2 FTIR spectra of LCPi/SiO_2 (1.5 wt %) hybrid films.

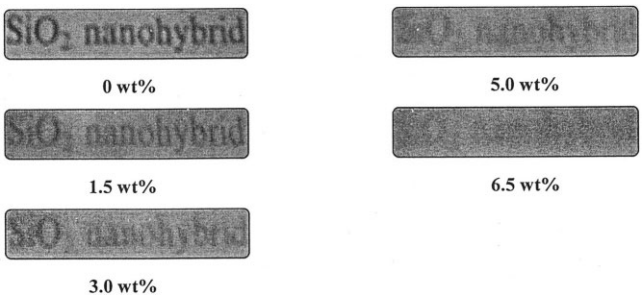

Figure 3 Appearance of LCPi and LCPi/SiO_2 hybrid films.

stirred at 150–155°C for 24 h at the reflux condition. Then it was filtered under hot condition. The filtrate was cooled to the ambient temperature. The yellow precipitate was filtered out and washed with ethyl alcohol. Then, it was dried at 70°C for 12 h. The yield of 1,3-bis[4-(4′-nitrophenoxy)cumyl]benzene (BNCB) was 23 g (73%). The synthesis process of BNCB monomer is shown in Scheme 1.

Elemental analysis calculated for BNCB ($C_{36}H_{32}N_2O_6$): C 73.45%, H 5.48%, N 4.76%. Found: C 73.02%, H 5.49%, N 4.90%; IR (K Br, cm^{-1}): 1500, 1352 cm^{-1} (—NO_2), 1267 cm^{-1} (C—O—C). ^1H NMR (d-chloroform, ppm, δ): 1.69 ppm (Ar-H), 6.96–820 ppm (—CH_3). T_m: 148.5–153.5°C.

Synthesis of 1,3-bis[4-(4′-amino-phenoxy)cumyl]benzene (BACB)

Dinitro (BNCB, 11.76 g, 0.02 mol), ethyl alcohol (50 mL), and 5% palladium on activated carbon (catalyst, 0.5 g) were added to a 100 mL three-necked flat flask equipped with a stirrer (a vacuum closed vessel). The mixture was stirred and heated to reflux for 10 min, and then the hydrazine monohydrate (7 mL) was added dropwise via an addition funnel in 2.5 h. The reaction was maintained for 24 h. The catalyst was filtered off under the hot condition. After cooling to the ambient temperature, the precipitated white powder was filtered and washed with deionized water, followed by drying at 70°C for 12 h. The yield of 1,3-bis[4-(4′-amino-Phenoxy)cumyl]benzene (BACB) diamine was 10 g (85%). The synthesis process of BACB monomer is shown in Scheme 2.

Elemental analysis calculated for BACB ($C_{36}H_{36}N_2O_2$): C 81.79%, H 6.86%, N 5.30%. Found: C 81.69%, H 6.86%, N 5.22%; IR (K Br, cm^{-1}): 3423, 3344 cm^{-1} (—NH_2), 1267 cm^{-1} (C—O—C). ^1H NMR (d-chloroform, ppm, δ): 1.63 ppm (Ar-H), 6.66–7.27 ppm (—CH_3), 3.57 ppm (—NH_2). T_m: 103.5–105.5°C.

Preparation of LCPi/SiO_2 hybrid films

A 100 mL three-necked flat-bottom flask containing equimolar amount of BACB diamine (2.512 g) and 20 mL of DMAC were stirred for 30 min–1 h at the room temperature. Then, 1.0167 g of PMDA was added. The mixture was stirred at room temperature for 24 h to gain a yellowish viscous liquid crystalline polyamic acid (LCPAA) solution. Then, TEOS and ethanol were added after being stirred for 4–8 h at room temperature. The amount of TEOS–ethanol was decided by the SiO_2 content desired in the hybrid. After the addition of TEOS–ethanol solution, further stirring was needed to recover a homogeneous solution. The yellow transparent solution was spin-coated onto the slide glass plate and dried at 60°C for 1 h. The films were heated, respectively, at 80, 100, 150, 200, and 250°C for 1 h through thermal imidization process, as shown in Figure 1. The thickness of the imidized films was about 50 μm, and the films were peeled off the glass substrates with the aid of deionized water and dried for several hours at 100°C in a vacuum oven. The formulations for the LCPi/SiO_2 hybrids discussed in this article are shown in Table I. The synthesis process of LCPAA solution and preparation of LCPi/SiO_2 hybrid films by sol–gel process are shown in Schemes 3 and 4. T_m: 350–360°C.

Measurements

Nuclear magnetic resonance (^1H NMR) spectra of BNCB and BACB were measured with a Bruker DMX-500 MHz FT-NMR. Elemental analysis of BNCB and BACB were measured with a Heraeus VarioEL-III type (Germany). Fourier transform infrared (FTIR) spectra of LCPi and LCPi/SiO_2 hybrid films were recorded on a Nicolet MAGNA-IR 550 spectrometer. The liquid crystalline texture was observed with the use of an Olympus DP-12 microscope (polarizing optical microscopy; POM) coupled with a MEEELER FP90 Central Processor (FP82HT Hot Stage). The morphology of the cross section was investigated by high resolution field-emission scanning electron microscope (FESEM) with a JSM-6500F (JEOL, Japan). The LCPi and LCPi/SiO_2 hybrid films were performed at room temperature on an MXP18 (MAC Sience, Japan) X-ray powder diffractometer, using Ni-filtered Cu Kα radiation. The scanning rate was 4°/min over a range of $2\theta = 2°–60°$ and the operating voltage was 40 KV (30 mA). Thermogravimetric (TGA) analysis of LCPi and LCPi/SiO_2 hybrid films were carried out under a flow of N_2 atmosphere (20 cc/min) on Mettler TGA/

TABLE II
Transparency of LCPi and LCPi/SiO_2 Hybrid Films

Hybrid film	LCP type	Silica content (SiO_2 wt %) 0	1.5	3.0	5.0	6.5
1	BACB–PMDA	T	Tr	Tr	Tr	Tr

T, transparent; Tr, translucent.

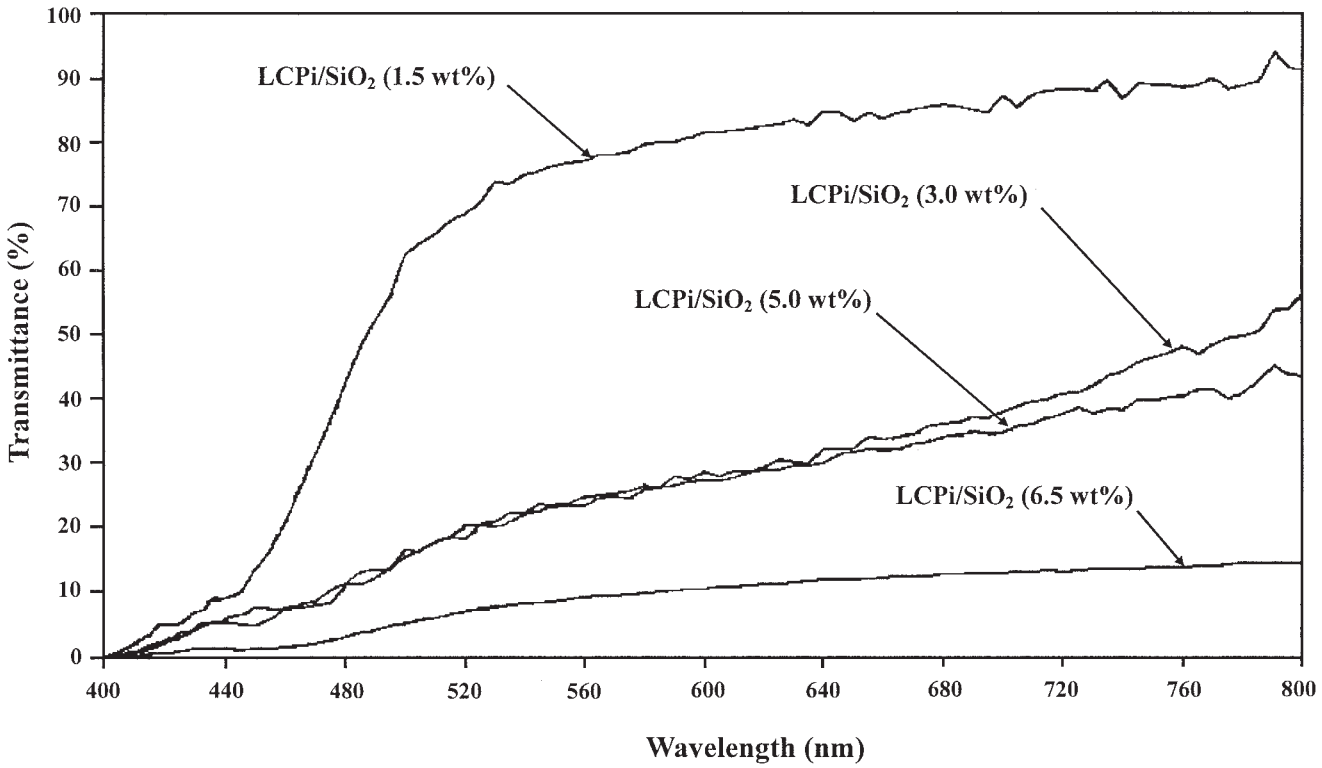

Figure 4 Transmittance of LCPi/SiO_2 hybrid films.

SDTA85e. The samples were heated and cooled at a rate of 10°C/min. The glass transition temperature (T_g) and the liquid crystal phase transition temperature of LCPi and LCPi/SiO_2 hybrid films were investigated with the Perkin-Elmer Pyris 1 (differential scanning calorimeter, DSC) instrument, under the N_2 atmosphere (20 mL/min), and at a heating rate of 20°C/min. Optical transparency analyses of LCPi/SiO_2 hybrid films were carried out with the Model TFM-120AFT (birefringence analyzer). The tensile strength of LCPi and LCPi/SiO_2 hybrid films was determined on a Micro-Computer Universal Testing Machine (Orientec Tensilon RTA-1T, AR-6000) at room temperature, with a drawing rate of 5 mm/min. The dielectric constant of LCPi and LCPi/SiO_2 hybrid films were measured at room temperature by an electrical analyzer (HP4192A).

RESULTS AND DISCUSSION

FTIR spectra of LCPi/SiO_2 hybrid films

Figure 2 shows the FTIR spectrum of a LCPi/SiO_2 hybrids containing 1.5 wt % SiO_2. The characteristic absorption bands of C═O at 1776 and 1728 cm^{-1}, C═C at 1600 and 1502 cm^{-1}, $\diagdown\!\diagup$N— at 1383 cm^{-1}, C—O—C at 1242 cm^{-1}, Si—O—Si at 1092 cm^{-1}, aromatic ring at 1014 cm^{-1}, Si—OH at 941 cm^{-1}, and aromatic C—H at 881 and 823 cm^{-1} can be observed. These results indicate the presence of LCPi/SiO_2 hybrids.

Appearance of hybrid films

The appearance of the films was compared, as shown in Figure 3 and Table II. The transparency of LCPi and LCPi/SiO_2 (1.5, 3.0, 5.0, and 6.5 wt %) hybrid films were shown by a direct observation.

Optical transparency analysis

Most polyimide/SiO_2 hybrids are transparent to translucent hybrids, because the nanoparticle diameter is less than the wavelength of visible light (400–700 nm). When hybrids are produced with higher SiO_2 contents (>6.5 wt %), the phase separation becomes evident, leading to an opaque appearance. So, the

TABLE III
Transmittance of LCPi/SiO_2 Hybrid Films (at Wavelength of 800 nm)

LCPi/SiO_2 (wt %)	Transmittance (%)
1.5	≅91
3.0	≅57
5.0	≅44
6.5	≅14

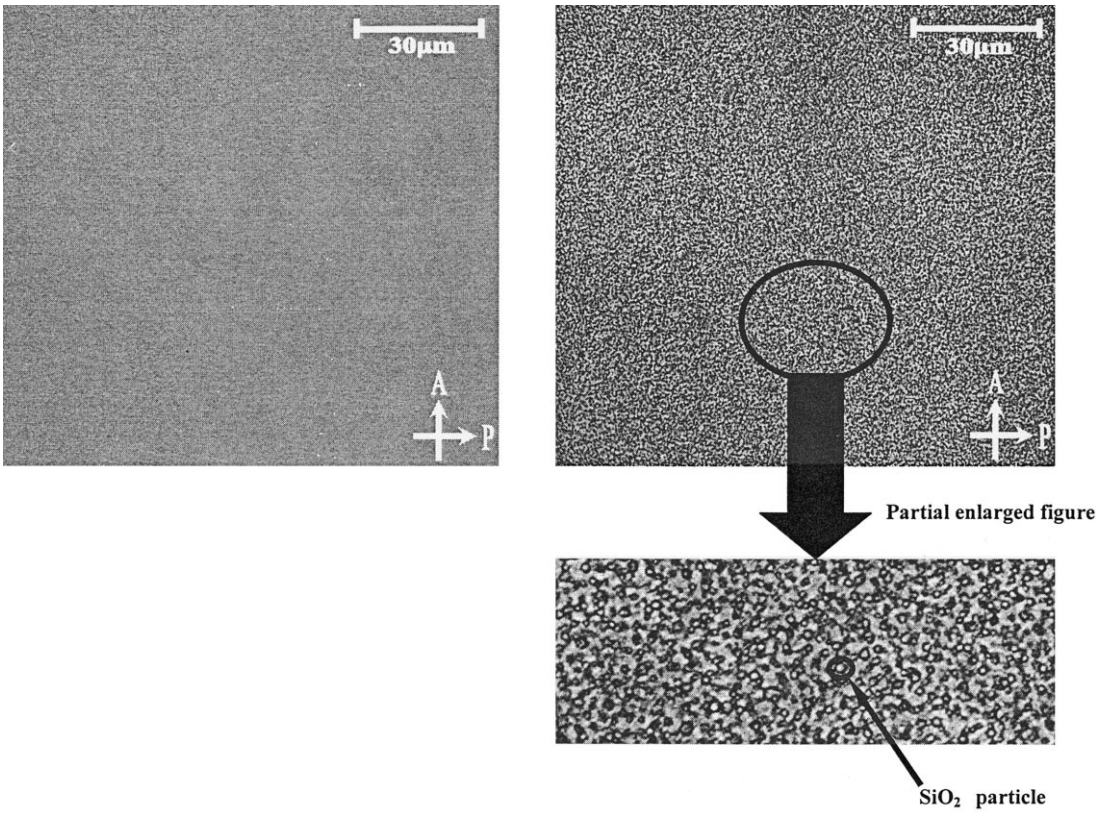

Figure 5 Appearance of LCPi and LCPi/SiO_2 hybrid films (a) LCPi (BACB–PMDA) and (b) LCPi/SiO_2 (6.5 wt %).

transparency of LCPi/SiO_2 hybrid films decreased with increasing SiO_2 content, as shown in Figure 4 and Table III.

POM analysis

The polarizing optical micrographs of LCPi and LCPi/SiO_2 hybrid films are shown in Figure 5. The LCPi film was highly transparent, as shown in Figure 5(a). When the SiO_2 content reached 6.5 wt % in the hybrid films, the size of inorganic particles increased up to 800–900 nm, resulting in a decrease in the transmittance of the film, as shown in Figure 5(b).

Liquid crystalline phase analysis

The liquid crystalline texture of this polyimide was observed via an Olympus DP-12 microscope coupled with an FP82HT hot stage. All samples were pressed between two glass slides on a hot plate at 330°C. They were quenched at a heating rate of 10°C/min and to the room temperature in air before observation. The nematic phases of LCPi and LCPi/SiO_2 were not observed. The Smectic A phase texture of LCPi at 294.9°C is shown in Figure 6.

XRPD analysis of hybrids

Liquid crystalline phase analysis

XRPD (X-Ray Powder Diffractometer) powder pattern displays a sharp diffraction peak of LCPi and LCPi/SiO_2 hybrid films at a lower angle (Fig. 7). It also confirms that it is a smectic A phase liquid crystal.[4]

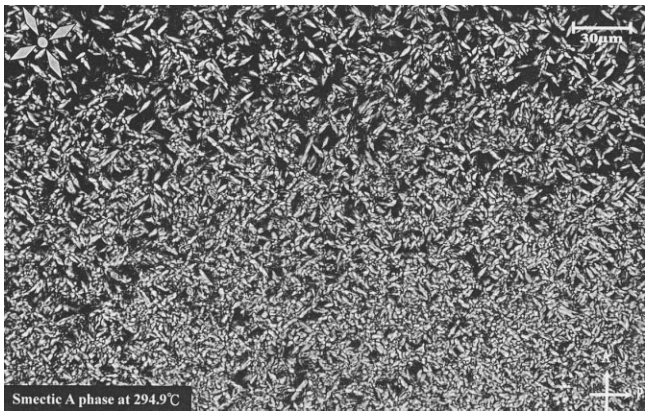

Figure 6 Polarizing optical micrographs of LCPi (Smectic A phase texture).

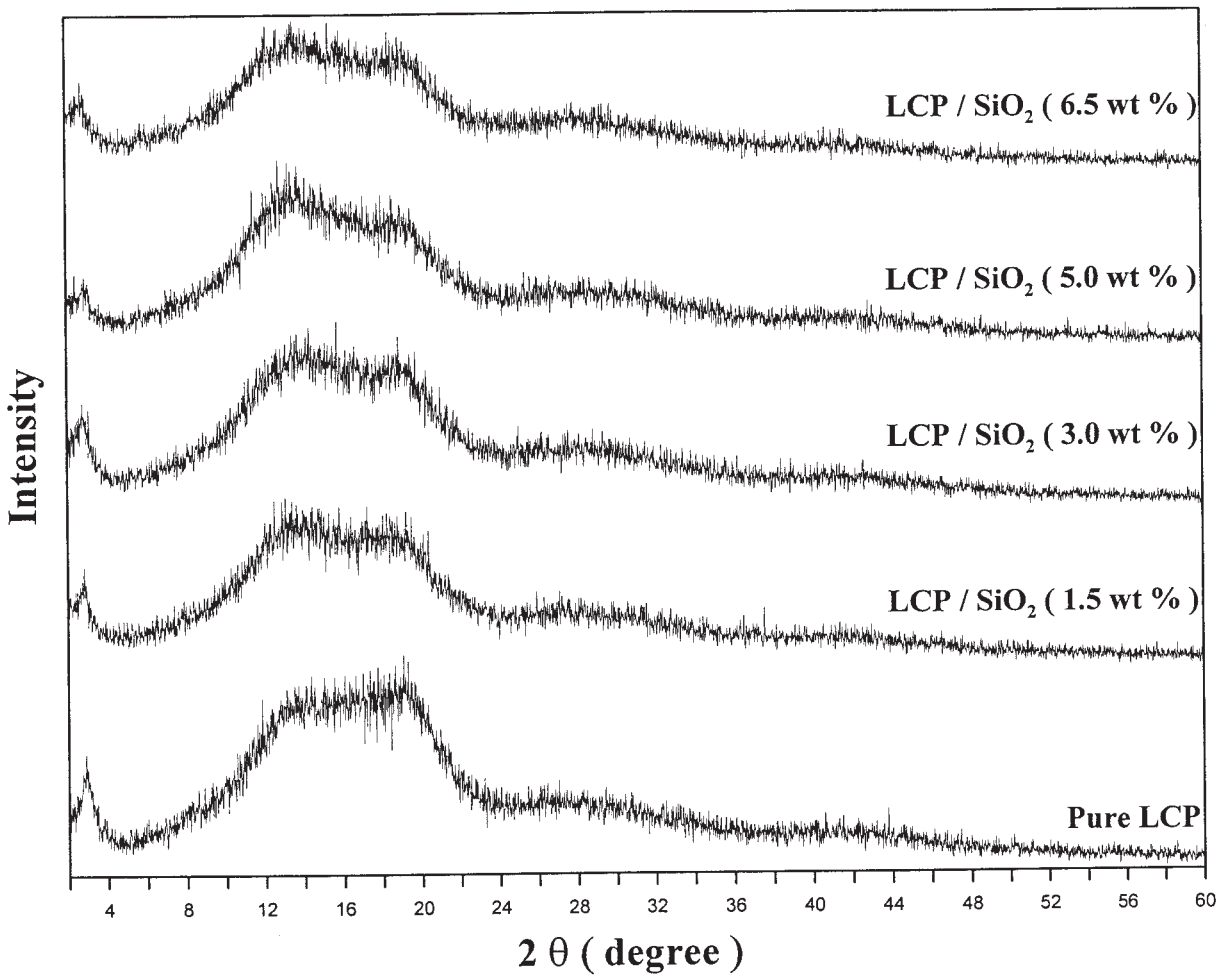

Figure 7 XRPD powder pattern of LCPi and LCPi/SiO_2 hybrid films.

Crystalline of LCPi and LCPi/SiO_2 hybrids analysis

Figure 7 shows the XRPD powder pattern. We can fundamentally observe that the diffraction peak of LCPi is broader. Therefore, it can be used to determine that the order of molecular orientation of LCPi is poor. It belongs to an unset liquid crystalline polymer, and the molecules have no orientation. So, it is generally assured that the synthesized LCPi is an amorphous liquid crystalline polymer. Besides adding SiO_2 particle to LCPi, as shown in Figure 7, the SiO_2 particle does not have any influence on the order of molecular orientation of LCPi, and also with the increase of SiO_2, it has no effect on the crystallization of LCPi, and all the diffraction peaks were broadened.

FESEM analysis of LCPi and LCPi/SiO_2 hybrids

The FESEM photographs provided us with an important information on the morphology of the LCPi and LCPi/SiO_2 hybrid films. Figures 8(a)–8(e) show the FESEM photographs of the cross sections of the LCPi and LCPi/SiO_2 (1.5–6.5 wt %) hybrid films. The dispersed SiO_2 particles could be seen as white beads with varying diameters in the range of 400–900 nm. When the SiO_2 content was below 3.0 wt %, the SiO_2 particle size was about 377 nm. However, when the SiO_2 content was increased to 3.0–6.5 wt %, the particle size was increased to 577–832 nm, respectively. The increase in the SiO_2 particle size clearly resulted in an increase in the aggregation tendency and phase separation as the SiO_2 content were increased. The particle size increased with increase in the SiO_2 content. So, when the SiO_2 particles was with a diameter less than the wavelength of visible light (400–700 nm), it made the hybrid film transparent.

DSC analysis

The T_g's of the LCPi and LCPi/SiO_2 (3.0 wt %) hybrid films detected by differential scanning calorimetry (DSC) are shown in Figure 9(a) and 9(b) and Table IV. The addition of SiO_2 resulted in an increase in the hybrid film's T_g when the SiO_2 content was less than 6.5 wt %. In this system, the SiO_2 particles acted as

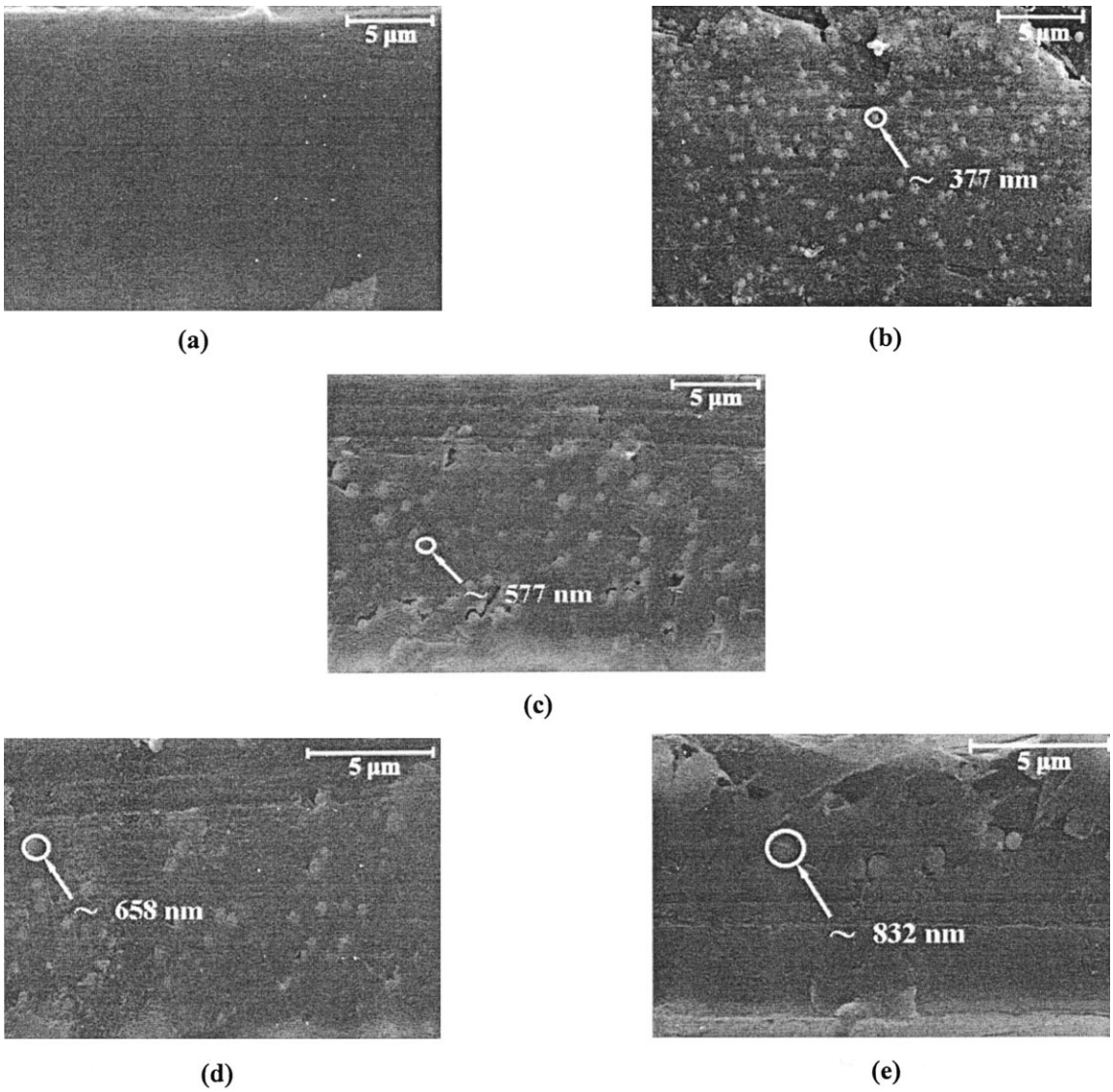

Figure 8 Photographs of Field-Emission Scanning Electron Microscope (FESEM) of LCPi/SiO_2 hybrid films. LCPi films containing (a) 0, (b) 1.5, (c) 3.0, (d) 5.0, and (e) 6.5 wt % of SiO_2.

physical crosslink points, which limited the movement of the molecular chain of LCPi.

This liquid crystalline polyimide exhibited a normal melting peak around 275°C and transformed into a smectic A phase. The smectic A phase changed to a nematic phase upon heating to 298°C, and then it turned into an isotropic melt around 350°C.[9] The thermal analysis curves for LCPi and LCPi/SiO_2 during the second heating process starts from 25 to 370°C, with a heating rate of 10°C/min. The LCPi has a thermotropic liquid crystalline phase at 275.73°C for Smectic A phase and 297.90°C for Nematic phase. The LCPi/SiO_2 (3.0 wt %) have a thermotropic liquid crystalline phase at 274.44°C for Smectic A phase and 300.23°C for Nematic phase. The temperature of liquid crystalline phase (LC phase) appeared as shown in Figure 9(a) and 9(b), and Table V.

Thermal stability of LCPi and LCPi/SiO_2 hybrids

Figure 10 shows the thermogravimetric curves of the LCPi and LCPi/SiO_2 hybrid films with different SiO_2 contents. The sample exhibits a very good thermal stability before 400°C. It begins to decompose around 420–430°C in N_2 gas. The 5% weight loss temperature is about 527.63°C. For the POM and DSC experiments, no decomposition could be considered because the operating temperature was below 400°C. The LCPi had a high decomposition temperature (T_d, on-set temperature) of about 527.63°C. This thermal stability was further improved when SiO_2 was introduced. The LCPi/SiO_2 hybrid films containing 6.5 wt % SiO_2 had a T_d of 570.27°C, as shown in Table VI. The thermal stability of the LCPi/SiO_2 hybrids increased upon in-

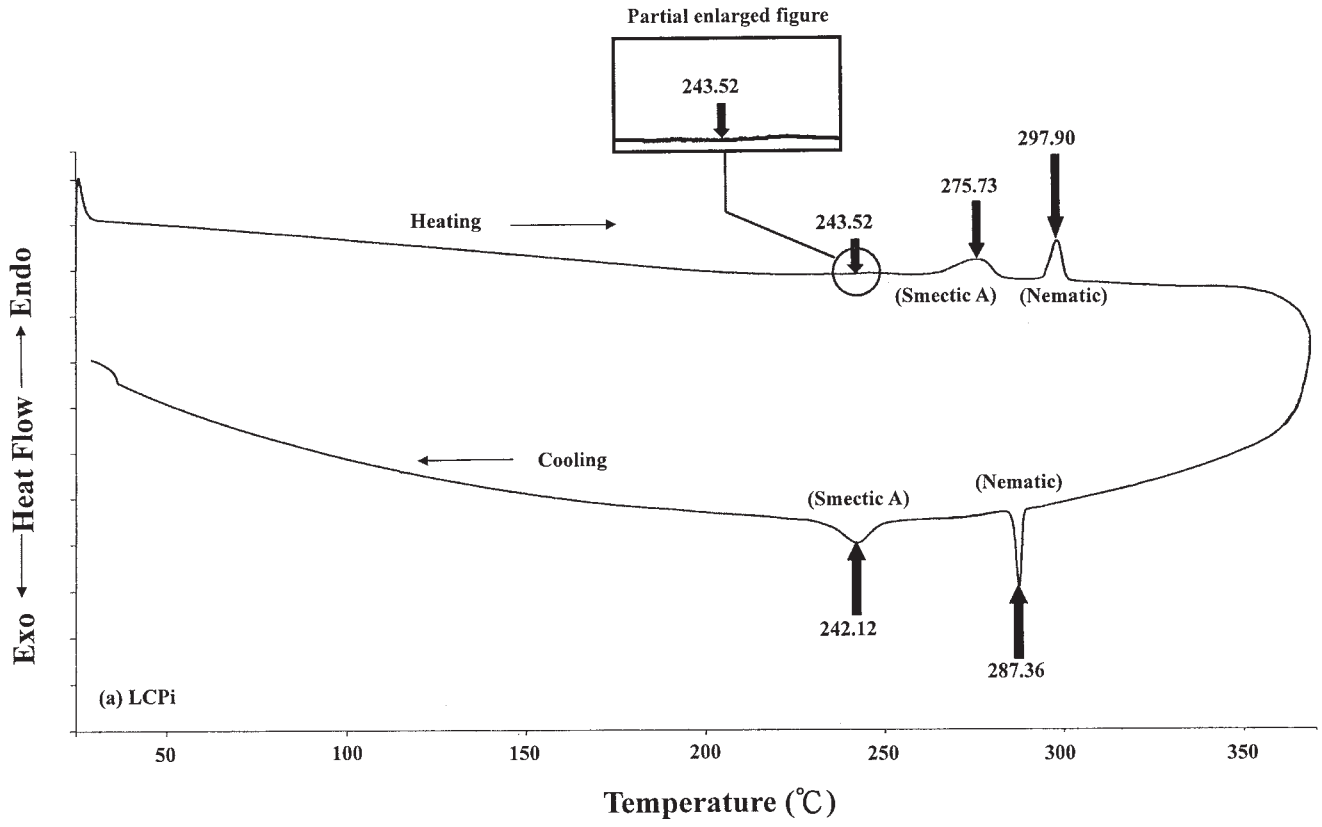

(a)

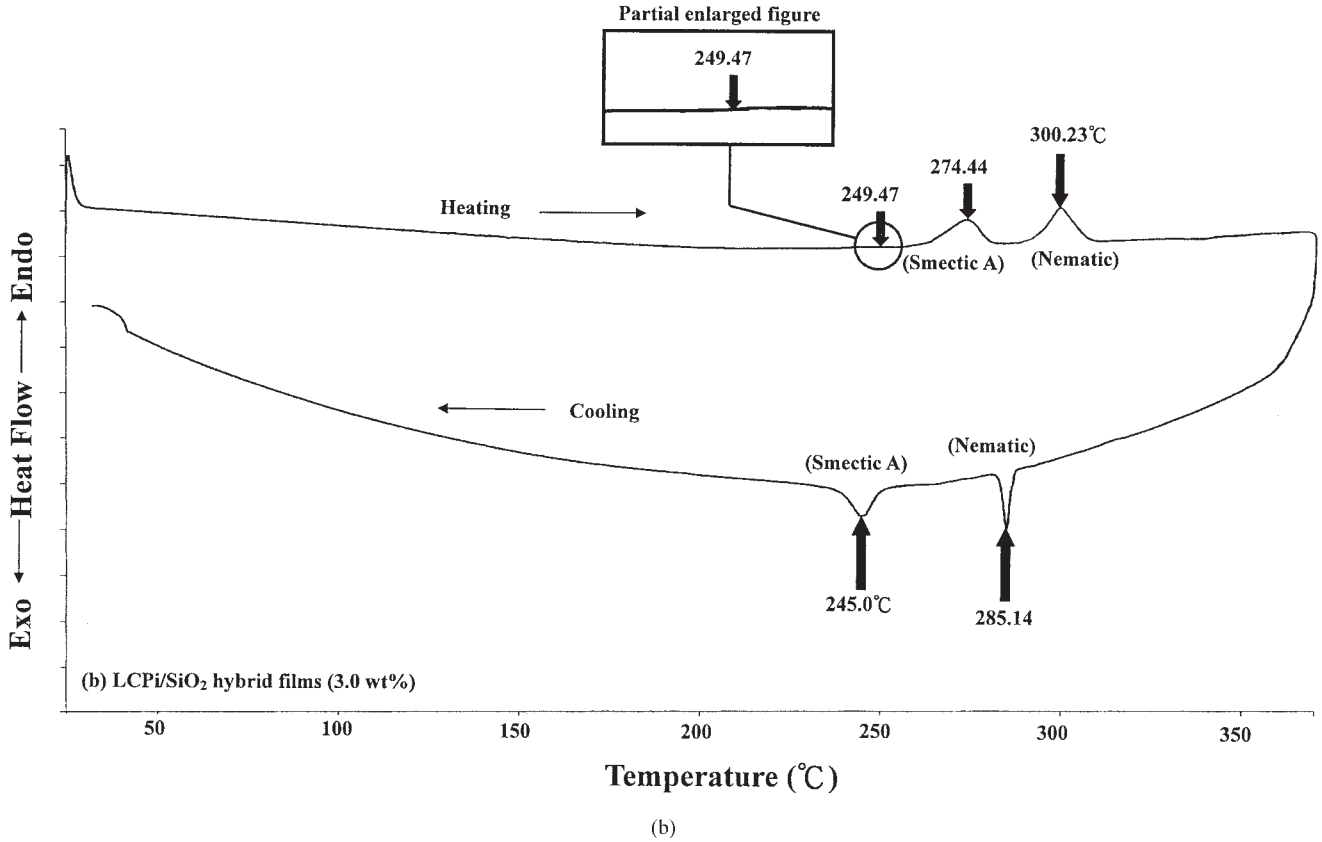

(b)

Figure 9 DSC thermograms for the second heating and second cooling of (a) LCPi and (b) LCPi/SiO_2 (3.0 wt %) hybrid films.

TABLE IV
Effect of SiO_2 Composition on the T_g of LCPi and LCPi/SiO_2 Hybrid Films

Sample	T_g (°C)
Pure LCPi	243.52
LCPi/SiO_2 (1.5 wt %)	249.03
LCPi/SiO_2 (3.0 wt %)	249.47
LCPi/SiO_2 (5.0 wt %)	249.68
LCPi/SiO_2 (6.5 wt %)	241.76

TABLE VI
The Temperature of Decomposition of LCPi and LCPi/SiO_2 Hybrid Films

Sample	T_d (in nitrogen °C)[a]
Pure LCPi	527.63
LCPi/SiO_2 (1.5 wt %)	539.19
LCPi/SiO_2 (3.0 wt %)	545.14
LCPi/SiO_2 (5.0 wt %)	553.51
LCPi/SiO_2 (6.5 wt %)	570.27

[a] Thermal decomposition temperature of 5 wt % loss of hybrid film obtained from TGA.

creasing the SiO_2 content. This increase in the thermal stability may result from the high thermal stability of SiO_2 network and the physical crosslink points of the SiO_2 particles, which limited the movement of the molecular chain of LCPi.

The function of adding SiO_2 particle to LCPi is due to its high thermal stability and high melting point, up to 1600°C. After adding nano-SiO_2 particles with high melting point to the polymer matrix, the SiO_2 particles can serve as a good thermal cover layer, avoiding the direct thermal decomposition of polymer matrix by heat. In addition, the SiO_2 is a nanoscale particle, and so it can provide the thermal cover layer, which offers a larger surface area and improves the effect of thermal cover.

Nevertheless, below 1000°C, N_2 environment, the TGA analysis of LCPi is still left at about 38.5 wt %. Theoretically, almost all organic materials are burned out at 1000°C; therefore, it is impossible for organic materials to be left so much. In fact, the reason is that the sample is more stable under N_2 environment than in air environment, and the surface of the sample forms a layer of char at high temperature. This is to say that the sample is wrapped by char, and char has a flame-retardant effect. Therefore the sample does not burn out at high temperature.

Mechanical properties of the hybrid films

Mechanical tester is with a tension rate of 5 mm/min. Figure 11 shows the influence of the SiO_2 content on the tensile strength and elongation at the breakage of the LCPi and LCPi/SiO_2 hybrid films. The tensile strength (failure) increased with the SiO_2 content up to 5 wt %. The tensile strength at break was increased by about 19% when 5 wt % SiO_2 was introduced, and the elongation at the breakage decreased with increase in the SiO_2 content. Such strengthening and brittling effects might have resulted from the strong interaction and the interpenetration between the LCPi molecules and SiO_2 network, that is, which may result from the strong physical interaction between organic and inorganic phases, leading the formation of the "Physical crosslinks". The strength and the brittleness of the hybrid were certainly dependent upon the density of the crosslinks. At an appropriate range of the crosslink density, the crosslinks could exhibit the strengthening and brittling effects. Figure 12 shows the influence of the SiO_2 content on the modulus at break of the hybrids. The modulus at break increased linearly with the increase of the SiO_2 content. In addition, the unique mechanical behavior of LCPi/SiO_2 hybrid films resulted mainly from a good dispersion, strong Si—O bonds in the SiO_2 particles, and interfacial adhesion of SiO_2 particles when the SiO_2 content was lower than 6.5 wt %. Table VII shows the mechanical properties.

Electrical analysis of LCPi and LCPi/SiO_2 hybrids

Figure 13 shows the effect of SiO_2 contents on the dielectric constant (ε_r) of the LCPi and LCPi/SiO_2 hybrid films. The dielectric constants (at 300 mV, 1 MHz) of the hybrid films decreased with increase in the SiO_2 content. The dielectric constants of the LCPi and LCPi/SiO_2 hybrid films ranged from 3.43 to 2.48. The dielectric constant was decreased by about 27.69% when 6.5 wt % SiO_2 was introduced.

TABLE V
The Temperature of Liquid Crystalline Phase of LCPi and LCPi/SiO_2 Hybrid Films

Sample	Smectic A (°C)		Nematic (°C)	
	Heating	Cooling	Heating	Cooling
Pure LCPi	275.73	242.12	297.90	287.36
LCPi/SiO_2 (1.5 wt %)	272.55	247.64	301.41	291.70
LCPi/SiO_2 (3.0 wt %)	274.44	245.00	300.23	285.14
LCPi/SiO_2 (5.0 wt %)	274.72	241.20	300.74	289.42
LCPi/SiO_2 (6.5 wt %)	275.78	244.79	302.64	284.99

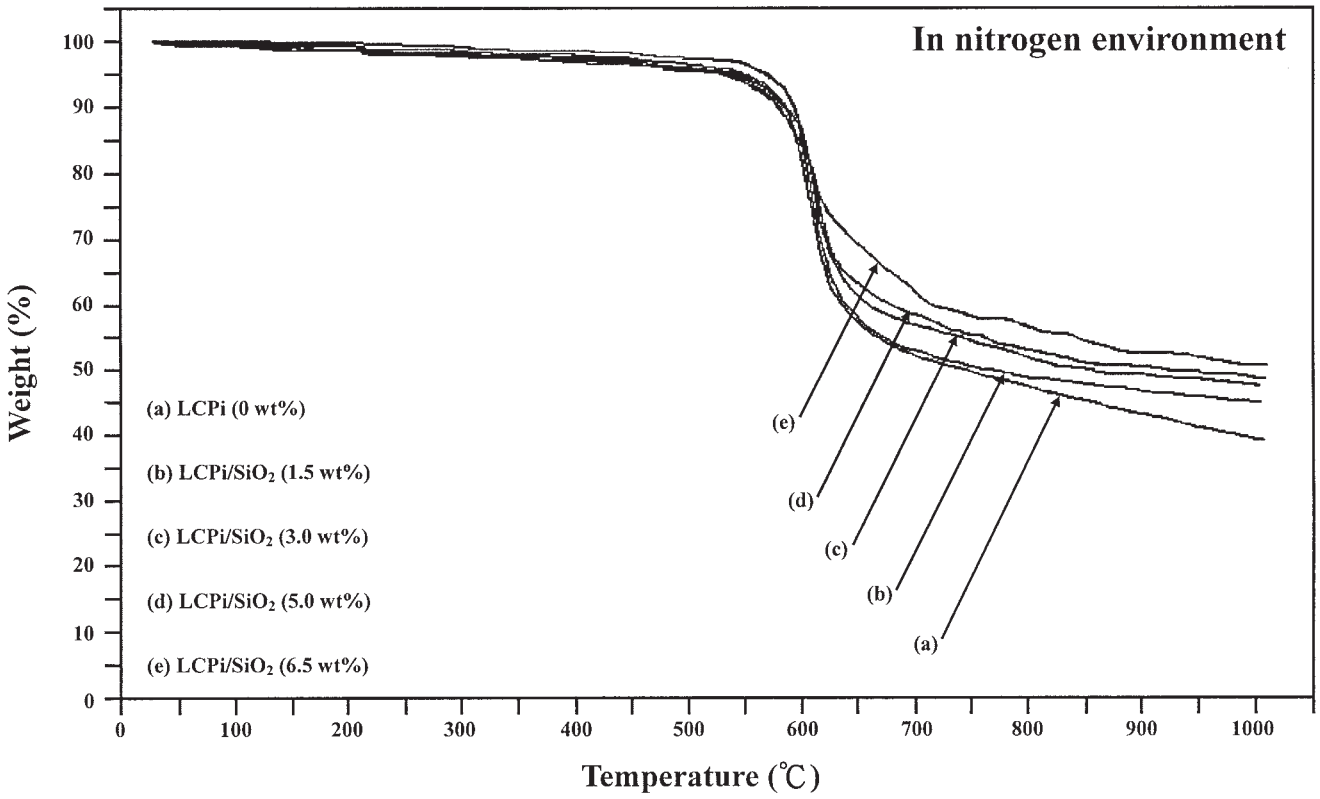

Figure 10 TGA curves of LCPi and LCPi/SiO_2 hybrid films.

The effect of SiO_2 contents on the surface resistivity (R_S) and volume resistivity (ρ_V) of the LCPi and LCPi/SiO_2 hybrid films are shown in Figures 14 and 15. The surface resistivity and volume resistivity of the hybrid films increased with increase in SiO_2 content.

Dense packing is necessary for the formation of the ordered structures required for intermolecular charge transfer. Therefore, in the LCPi/SiO_2 hybrid films, the SiO_2 acted as a hindrance, which reduced the possibility for the liquid crystalline polymer chain to form

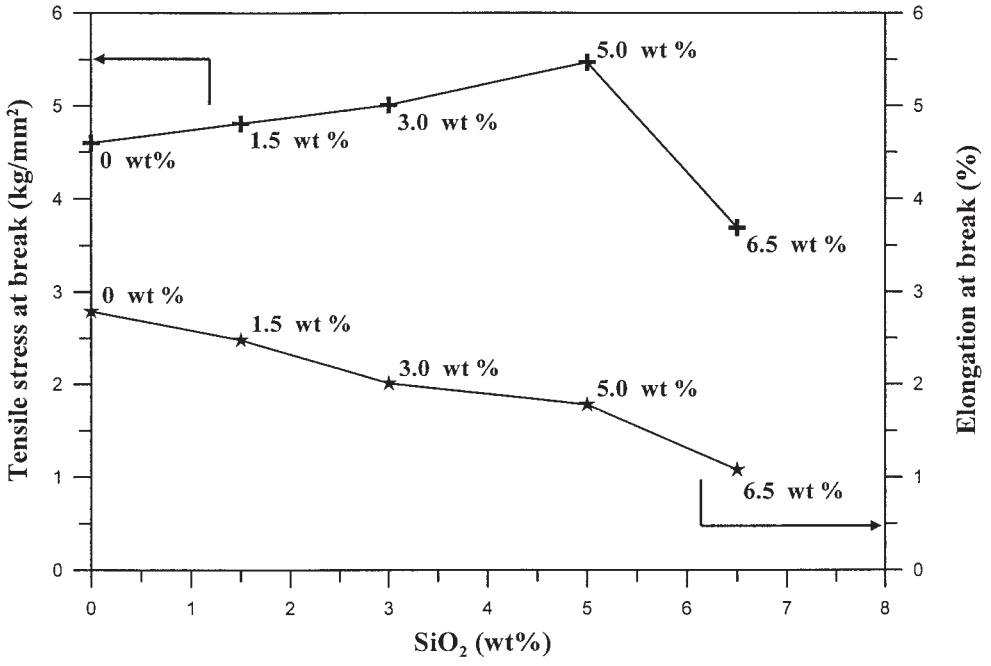

Figure 11 The tensile stress and elongation at break of the LCPi and LCPi/SiO_2 hybrid films.

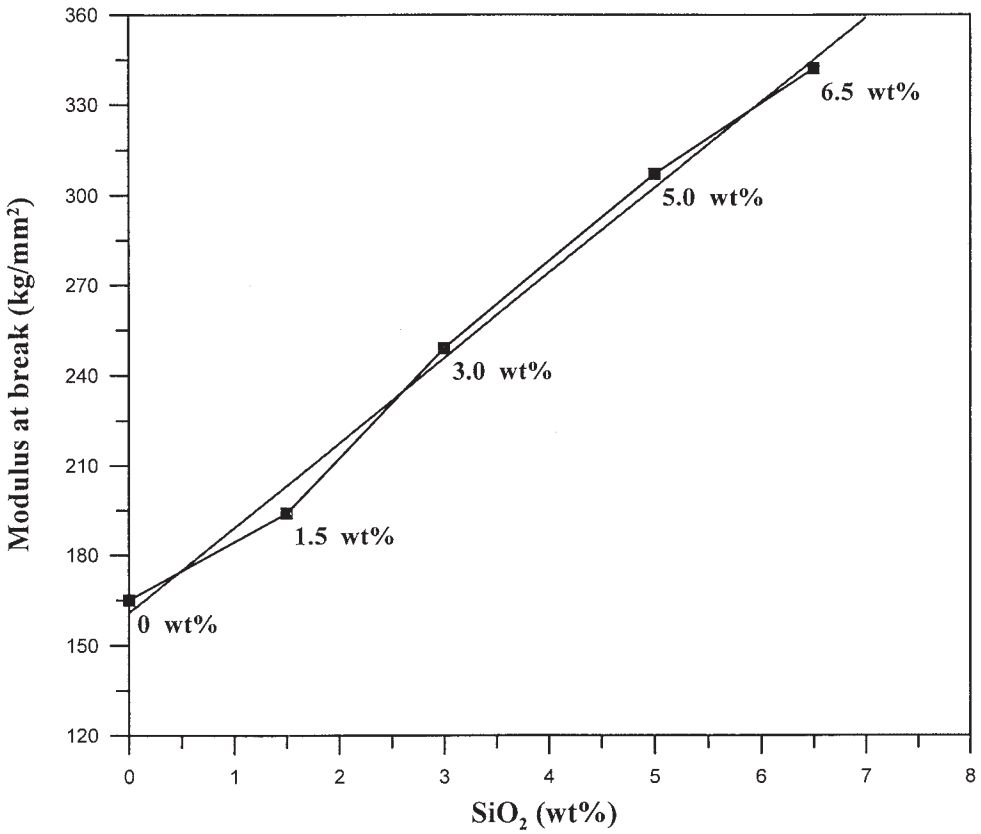

Figure 12 The Young's modulus of the LCPi and LCPi/SiO_2 hybrid films.

the well-packed donor/acceptor pairs.[22] So, the decrease of dielectric constant and increase of surface resistivity as well as volume resistivity were possibly caused by the inhibition of electrical treeing by SiO_2 particles. But the LCPi synthesized in this study can be looked as an amorphous liquid crystalline polymer. Consequently, for the LCPi and LCPi/SiO_2 hybrid films, they all have lower dielectric constants.

Water absorption rate analysis

LCPi contains carbonyl groups and has unshared electron pairs, and so it can easily form hydrogen bonds with water. Experimental results show that the water absorption rates decreased with increasing SiO_2 content, as shown in Figure 16.

Preparing method: before the experiment, we put the LCPi and LCPi SiO_2 hybrid films to dry for several hours at 100°C in a vacuum oven to ensure dehydration. We took them out to measure their dry weight (W_1), and then put them into deionized water for 24 h. We then took them out, wiped the water on their surface, and recorded the weight (W_2) of the hybrid films after dipping them into deionized water. Then, the water absorption rate was calculated from the following formula.

TABLE VII
Mechanical Properties of the LCPi and LCPi/SiO_2 Hybrid Films

Sample	Tensile stress at break (kg/mm²)	Elongation at break (%)	Modulus at break (kg/mm²)
Pure LCPi	4.60	2.79	164.8
LCPi/SiO_2 (1.5 wt %)	4.81	2.48	194.0
LCPi/SiO_2 (3.0 wt %)	5.01	2.01	249.0
LCPi/SiO_2 (5.0 wt %)	5.47	1.78	307.5
LCPi/SiO_2 (6.5 wt %)	3.69	1.08	341.6

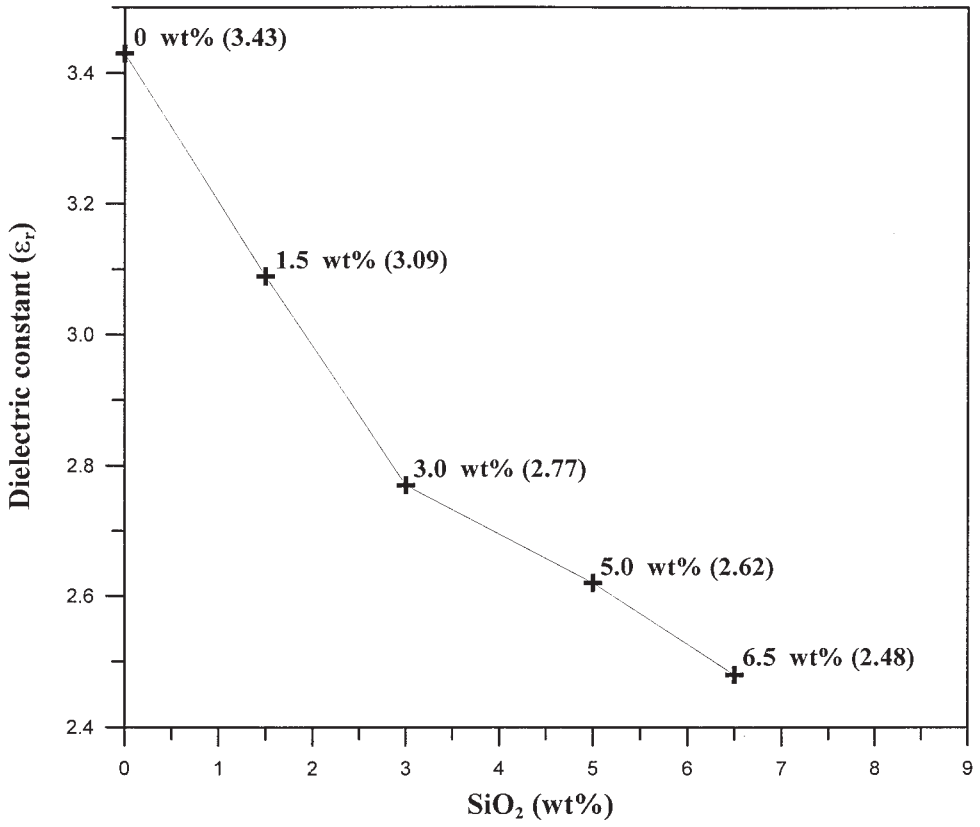

Figure 13 The dielectric constant (ε_r) of the LCPi and LCPi/SiO_2 hybrid films (at 300 mV, 1 MHz).

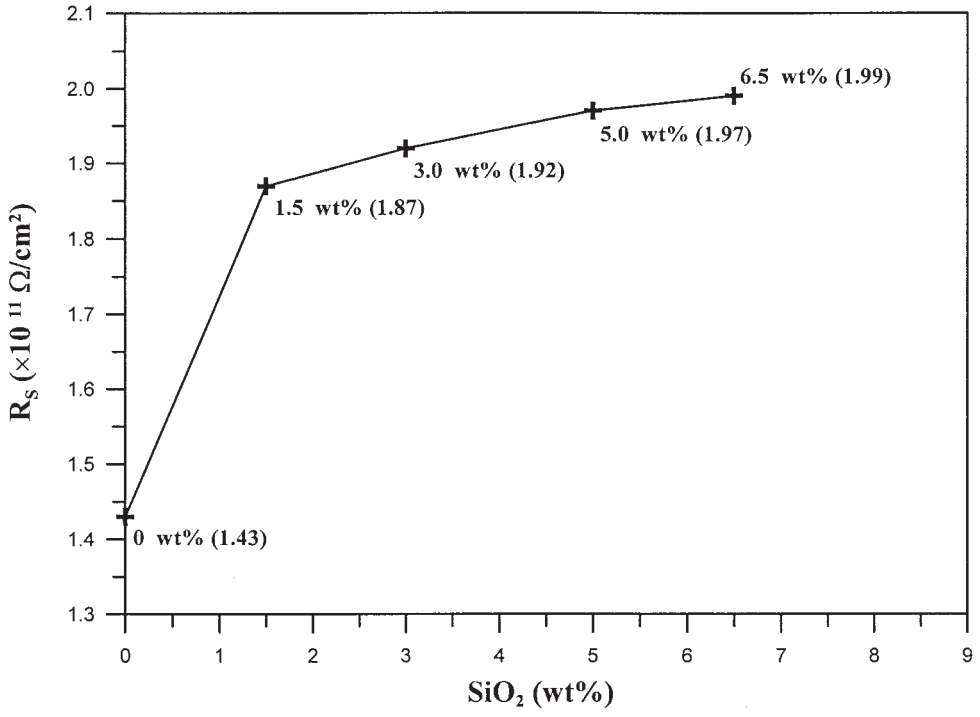

Figure 14 The surface resistivity (R_S) of the LCPi and LCPi/SiO_2 hybrid films.

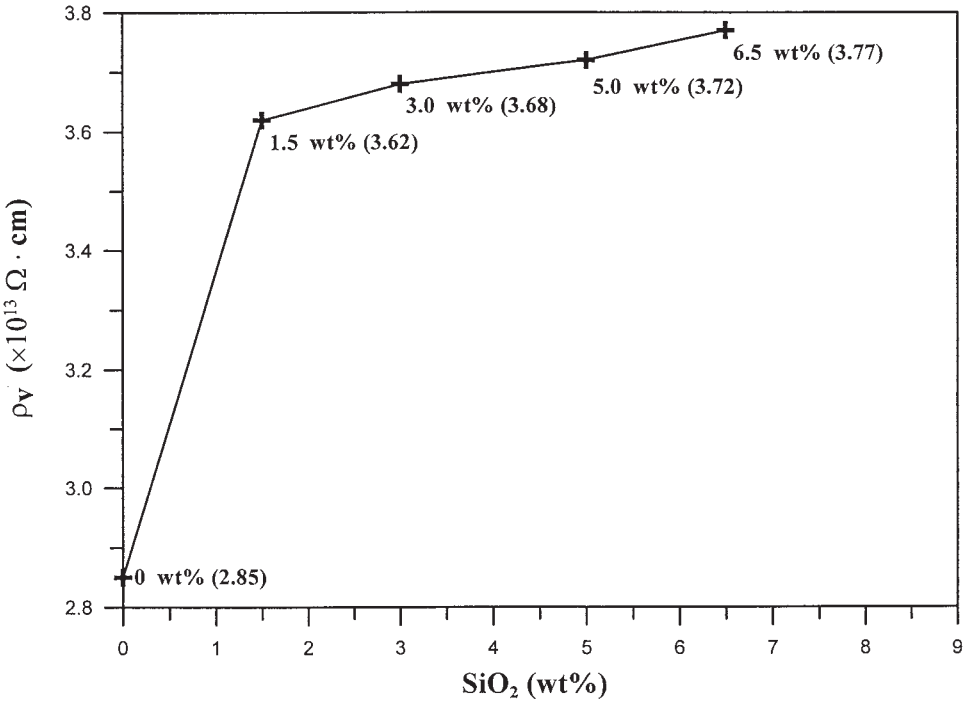

Figure 15 The volume resistivity (ρ_V) of the LCPi and LCPi/SiO_2 hybrid films.

$$\text{Water absorption rate (\%)} = \frac{(W_2 - W_1)}{W_1} \times 100\%$$

where W_1 is the weight of hybrid films before the water absorption and W_2 is the weight of hybrid films after the water absorption.

CONCLUSIONS

The main-chain-type thermotropic liquid crystalline polyimide was synthesized via a sol–gel process. Sol–gel processing was a good method for the preparation of LCPi/SiO_2 nanocomposites, which could avoid ag-

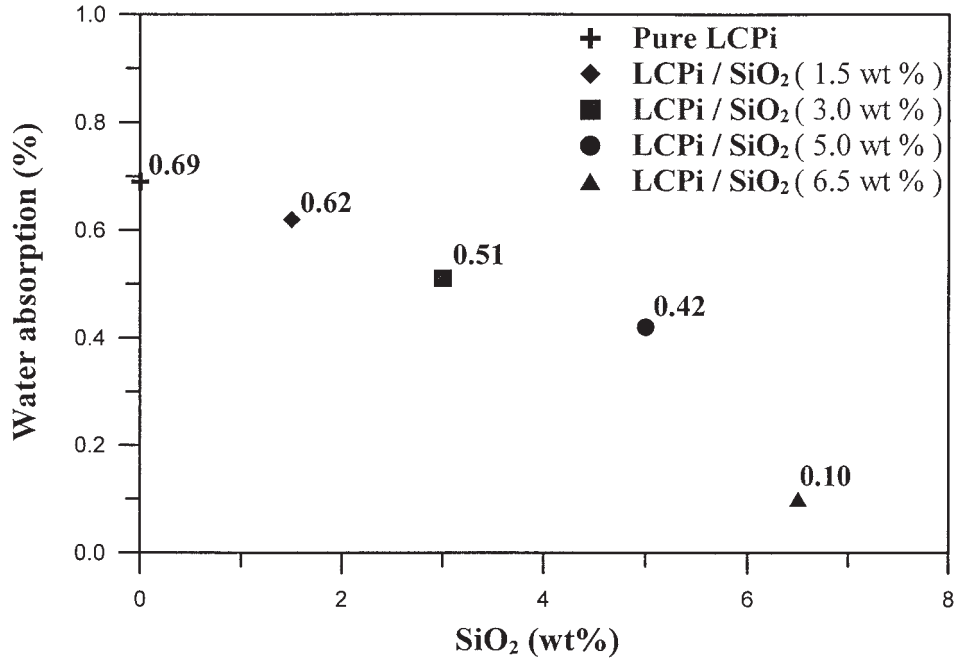

Figure 16 Water absorption rate of the LCPi and LCPi/SiO_2 hybrid films.

gregation of the SiO_2 particles in the polymer matrices. The transparency of hybrid films decreased with increase in SiO_2 content. The aromatic thermotropic liquid crystalline polyimide exhibits a smectic A texture above the melting temperature. The XRPD power pattern displays the LCPi and LCPi/SiO_2 hybrid films at a lower angle, which also confirms that it is a smectic liquid crystal (Smectic A phase), and LCPi can be looked as an amorphous liquid crystalline polymer. The FESEM observation showed that SiO_2 particles having a diameter of 400–900 nm dispersed homogeneously in the organic matrix. The SiO_2 particle size was about 400 nm for the hybrids containing 1.5 wt % SiO_2 and it increased with the increase of the SiO_2 content. The tensile stress at break of LCPi/SiO_2 hybrid films increased with the addition of SiO_2 and reached a maximum value when the SiO_2 content was up to 5.0 wt %. The strength of LCPi/SiO_2 hybrid films was improved simultaneously at a certain silica content range. The thermal stability and modulus at break of the hybrid films were also increased with the increase of the SiO_2 content. The dielectric constant of the LCPi and LCPi/SiO_2 hybrid films decreased with increase in SiO_2 content, and the surface resistivity, volume resistivity of the hybrid films increased with increase in SiO_2 content. The water absorption rates decreased with increase in SiO_2 content.

The author thanks the instrument center at the National Taiwan University (NTU), National Tsing Hua University (NTHU), National Taiwan Normal University (NTNU), and Graduate School of Materials Science Technology of NTUST for the helpful discussion and instrumental support.

References

1. Pramoda, K. P.; Chung, T. S.; Liu, S. L.; Oikawa, H.; Yamaguchi, A. Polym Degrad Stab 2000, 67, 365.
2. Chang, J. H.; Seo, B. S.; Hwang, D. H. Polymer 2002, 43, 2969.
3. Hsieh, T. T.; Tiu, C.; Simon, G. P. J Appl Polym Sci 2001, 82, 2252.
4. Liu, S. L.; Chung, T. S.; Lu, L.; Torh, Y.; Oikawa, H.; Yamaguchi, A. J Polym Sci Part B: Polym Phy 1998, 36, 1679.
5. Tamai, S.; Ohkawa, Y.; Yamaguchi, A. Polymer 1997, 38, 4079.
6. Tamai, S.; Oikawa, H.; Ohta, M.; Yamaguchi, A. Polymer 1998, 39, 1945.
7. Asanuma, T.; Oikawa, H.; Ookawa, Y.; Yamasita, W.; Matsuo, M.; Yamaguchi, A. J Polym Sci Part A: Polym Chem 1994, 32, 2111.
8. Junge, Z.; Baoyan, Z.; Yanying, W.; Zhiliu, F. J Appl Polym Sci 2001, 81, 2210.
9. Liu, S. L.; Chung, T. S.; Oikawa, H.; Yamaguchi, A. J Polym Sci Part B: Polym Phys 2000, 38, 3018.
10. Isayev, A. I.; Modic, M. Polym Comp 1987, 8, 158.
11. Huang, Y.; Gu, Y. J Appl Polym Sci 2003, 88, 2210.
12. Huang, J. C.; Zhu, Z. K.; Yin, J.; Zhang, D. M.; Qian, X. F. J Appl Polym Sci 2001, 79, 794.
13. Liu, J.; Gao, Y.; Wang, F.; Wu, M. J Appl Polym Sci 2000, 75, 384.
14. Kang, S. J.; Kim, D. J.; Lee, J. H.; Choi, S. K. Mol Cryst Liq Cryst 1996, 280, 277.
15. Kim, Y.; Kang, E.; Kwon, Y. S.; Cho, W. J.; Cho, C.; Chang, M.; Ree, M.; Chang, T.; Ha, C. S. Synth Met 1997, 85, 1399.
16. Wu, K. H.; Chang, T. C.; Wang, Y. T.; Chu, Y. S. J Polym Sci Part A: Polym Chem 1999, 37, 2275.
17. Schmidt, J. J. J Non-Cryst Solids 1988, 100, 51.
18. Nandi, M.; Conklin, J. A.; Salviati, J. L.; Sen, A. Chem Mater 1991, 2, 772.
19. Morikawa, A.; Lyiku, Y.; Kakimoto, M.; Imai, Y. Polym J 1992, 24, 107.
20. Sysel, P.; Maryska, M. Polym J 1997, 29, 607.
21. Lee, H. J.; Lin, E. K.; Wang, H.; Wu, W. L.; Chen, W.; Moyer, E. S. Chem Mater 2002, 14, 1845.
22. Khayankarn, O.; Magaraphan, R.; Schwank, J. W. J Appl Polym Sci 2003, 89, 2875.